Three-dimensional circulation of a mesoscale eddy/front system and its biological implications

PRIMO-0
Front
Mesoscale
Vertical velocity
Fertilization

PRIMO-0
Front
Méso-échelle
Vitesse verticale
Fertilisation

Jean-Michel PINOT [a], Joaquín TINTORE [a], José Luis LOPEZ-JURADO [b], Mari Luz FERNANDEZ DE PUELLES [b] and Javier JANSA [b]

[a] Departament de Física, Universitat de les Illes Balears, Palma de Mallorca, Spain.

[b] Instituto Español de Oceanografía, Centro Oceanográfico de Baleares, Palma de Mallorca, Spain.

Received 29/03/94, in revised form 28/02/95, accepted 2/03/95.

ABSTRACT

The three-dimensional circulation of an eddy/front system is quantified using hydrographic data collected in the Channel of Ibiza, Western Mediterranean, during November 1990. The ageostrophic motion is derived from the quasi-geostrophic omega equation. Maximum upward velocities (≈ 4 m/day) are diagnosed on the cold side of the front in the vicinity of a cyclonic eddy and coincident with a sub-surface convergence (below 50 m). This upward motion can be explained in terms of advection over isopycnals that uplift in the along-front direction. We also show the relevance of the three-dimensional circulation for the enhanced fertilization observed in the surface layer. Our results establish the importance of the ageostrophic dynamics induced by frontal mesoscale events for the regional ecology of the Balearic Sea.

RÉSUMÉ

La circulation tri-dimensionnelle d'un système front/tourbillon et ses implications biologiques.

La circulation tri-dimensionnelle d'un système front/tourbillon est quantifiée à partir de données hydrographiques acquises dans le Canal d'Ibiza (Méditerranée Occidentale) en novembre 1990. Le mouvement agéostrophique est calculé à l'aide de l'équation oméga quasi-géostrophique. Les vitesses verticales maximales (≈ 4 m/jour) sont diagnostiquées du côté froid du front, au voisinage d'un tourbillon cyclonique. Ces vitesses sont orientées du fond vers la surface et sont le produit d'une convergence au sein des couches sous-jacentes (en-dessous de 50 m). Ce déplacement vers la surface peut s'expliquer en terme d'advection le long d'isopycnes qui remontent vers la surface dans la direction du front. Nous montrons également que cette circulation tri-dimensionnelle favorise la fertilisation de la couche de surface. Nos résultats établissent l'importance de la dynamique agéostrophique induite par les perturbations frontales à méso-échelle pour l'écologie régionale en Mer Baléare.

Oceanologica Acta, 1995, **18**, 4, 389-400

INTRODUCTION

Recent experiments have shown that the study of fronts is particularly relevant in the Western Mediterranean, since they provide privileged biologically active locations in the general oligotrophic context of the Mediterranean Sea (Boucher *et al.*, 1987; Flos and Tintoré, 1990). The WMCE experiment (1985-87) established the importance of the frontal boundary regions between Mediterranean waters and waters of Atlantic origin for the increase of biomass in the Western Mediterranean (Lhorenz *et al.*, 1988). The ALMOFRONT-1 interdisciplinary experiment (1991) later focused on the Almeria-Oran front and assessed the effect of the frontal circulation on the ecosystem (Prieur and Sournia, 1994). Many studies specifically emphasized the strong spatial variability that characterizes nutrient and plankton distribution in frontal regions, suggesting a major influence of mesoscale processes. Examples of such a high variability in the Mediterranean Sea are given in Estrada and Margalef (1988) and Sabatés *et al.* (1989). In other regions of the world's oceans, it was demonstrated that maxima of nutrient concentrations were associated with frontal mesoscale structures such as filaments and eddies. This is the case for the cyclonic eddies of the tide-induced slope front over the Armorican continental shelf-break (Pingree *et al.*, 1979), but also for the mesoscale filaments of the wind-induced upwelling front in the California Current system (Brink and Cowles, 1991). Though many coupled physical/biochemical processes have been suggested, frontal mesoscale upwelling appears to be a major mechanism capable of accounting for the relationship between patchy distributions of enhanced biomass and mesoscale structures (Strass, 1992). Thus, in the case of the density fronts in the Western Mediterranean, the upward transport of nutrient-rich subsurface waters induced by frontal mesoscale upwelling is usually considered to be responsible for the fertilization of the euphotic layer and for the further enhanced phytoplankton concentrations which are measured in the vicinity of those fronts (Prieur, 1986; Tintoré *et al.*, 1988).

Ageostrophic vertical velocity is the critical parameter for diagnosing the strength and location of upwelling. Different methods are used to provide estimates of this variable (Fiekas *et al.*, 1994; Lindstrom and Watts, 1994). For the diagnostic of vertical motions from hydrographic data, the quasi-geostrophic omega equation (Hoskins *et al.*, 1978) has proved to be one of the most efficient techniques and has been successfully applied in several studies of fronts (Leach, 1987; Tintoré *et al.*, 1991; Pollard and Regier, 1992). The results obtained by Tintoré *et al.* (1991), who carried out objective analyses with scale separation and applied the quasi-geostrophic omega equation to hydrographic data collected in the Alboran Sea, are of particular interest since they established a relationship between the largest vertical velocities and the frontal mesoscale features. Those results have been confirmed by numerical studies (Barth, 1994; Strass, 1994).

The objective of this paper is to examine, in the case of the Balearic front, the effect of mesoscale distortions on frontal motions and to discuss their biological implications. The case-study described concerns a specific eddy/front system observed during the IBIZA-1190 experiment performed in the Channel of Ibiza in November 1990. First, the survey is described, then the hydrology and a geostrophic description of the eddy/front system are presented. Next, a quantitative estimate of the vertical velocity is produced by means of the quasi-geostrophic omega equation to characterize the ageostrophic frontal circulation. Finally, the biochemical observations are analyzed and the relevance of the diagnosed three-dimensional circulation for the fertilization of the upper layer is discussed.

The survey

The IBIZA-1190 experiment was performed by the Instituto Español de Oceanografía (IEO) to investigate the impact of the circulation on the biology in the Channel of Ibiza. This project was carried out within the framework of the PRIMO-0 programme. Six cross-channel hydrographic tran-

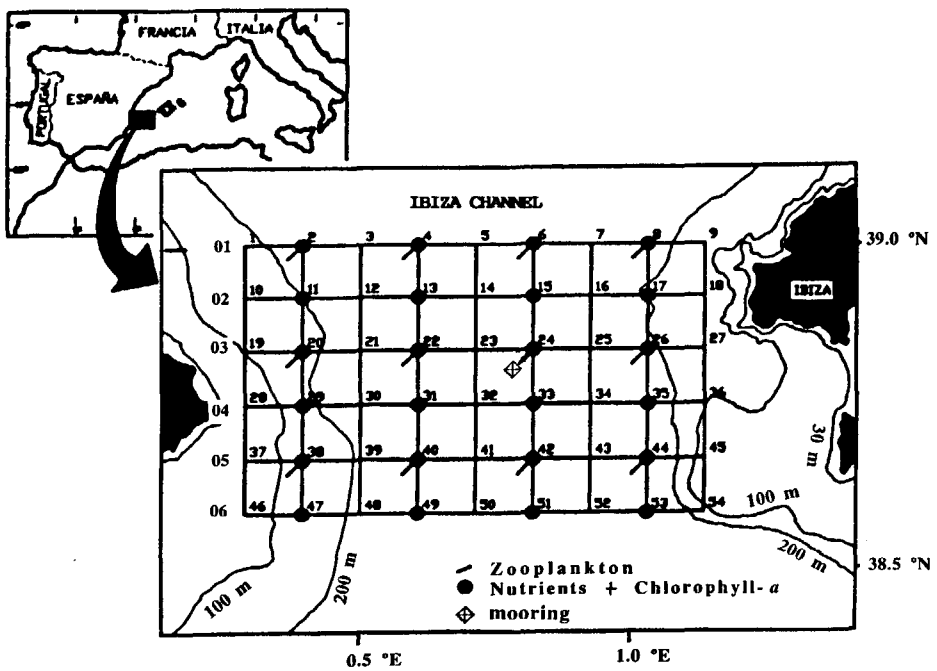

Figure 1

Morphology of the Channel of Ibiza and IBIZA-1190 sampling. Each node of the grid is one CTD station (Stations 1-54).

sects were performed from 15-19 November 1990, on board the Spanish R/V *Francisco de Paula Navarro* (Fig. 1). Thus, a total of 54 CTD casts were carried out in a quasi-synoptic manner by means of a Neil Brown MARK III probe. The mean distance between adjacent stations was about 9 km (Fig. 1). Procedures for CTD calibration and preliminary hydrographic analyses are given in López-Jurado *et al.* (1995). Nutrients (nitrates, nitrites, silicates and phosphates), dissolved oxygen and chlorophyll-*a* were measured in 24 of the 54 stations at standard depths (0, 25, 50, 100 and 200 m) by means of 3-l Niskin bottles (Fig. 1). Post-survey procedures as well as some preliminary discussion of the fertilization mechanisms are described in Jansá *et al.* (1992) and only a brief description is given here for completeness. Nutrient analyses were performed using a Technicon AAII autoanalyzer and nitrate concentrations were determined using the methodology of Armstrong *et al.* (1967) and Grasshof (1969). The chlorophyll-*a* concentration was deduced from fluorometric measurements using a Perkin-Elmer 204 spectrofluorometer. Mesozooplankton and microzooplankton data were collected at 12 of the 24 oxygen/nutrient/chlorophyll stations (Fig. 1). For microzooplankton, the sampling was performed using 32-l Niskin bottles at standard depths (0, 25, 50, 75 and 100 m). Water samples were filtered with a 45-μm net and the total number of individuals was further determined for each sample following the methodology described in UNESCO (1968) and Steedman (1976).

Hydrographic properties and geostrophic motions

Introduction

The Channel of Ibiza (maximum depth: 600 m) is one of the key passages of the Western Mediterranean that control the exchanges between the Balearic and Algerian basins. In the [0-150 m] surface layer of this channel, an energetic northward jet (the Balearic current) is generally observed over the Ibiza slope (Font *et al.*, 1988; Castellón *et al.*, 1990; García *et al.*, 1994). This flow transports light (warm and fresh) Modified Atlantic Waters (MAW) which generate an intense density front (the Balearic front) at their offshore boundary with the denser Mediterranean Waters (MW). This front is also found to the north, along the Balearic Islands slope. In a quasi-synoptic AXBT study, Pinot *et al.* (1994*a*) showed that the Balearic current/front was characterized by strong mesoscale distortions due to significant eddies and filaments. They also observed that, in the Channel of Ibiza, the topography/coast shape strongly constrained the flow, leading to enhancement of cross-channel gradients and along-channel velocities.

Vertical structure

Several cross-channel vertical sections of temperature, salinity, density and geostrophic velocity were constructed from the hydrographic profiles. Geostrophic velocities were obtained by first-differencing the dynamic height profiles between adjacent stations. Dynamic heights were computed through vertical integration of the specific volume anomaly from 250 m depth. A few stations in coastal areas of shallow depth (< 250 m) were extended downward by appending below them the dynamic height profile of the nearest deeper station. The 250 m no motion reference level was inferred from data obtained from Aanderaa current meters moored during the period 16 November 1990 - 24 July 1991 (Fig. 1). 250 m appeared as the depth where velocities were minimum (< 3 cm/s) (García-Lafuente *et al.*, 1995). At the time of the cruise, this depth corresponded to the interface between Levantine Intermediate Waters (LIW) and surface MAW and MW waters.

Vertical sections at transect 03 (Stations 19 to 27) are representative of the cross-front structure (Fig. 2*a-d*). In the upper 40 m, the thermal signature of the top of the front is masked by the presence of a seasonal summer thermocline [40-50 m] (Fig. 2*a*). Therefore, the best signature of the front is given by the salinity field (Fig. 2*b*). At 50 m, the front separates the MAW (S<37.0 psu) located over the Ibiza slope from the MW (S>38.0 psu) offshore. An isopycnal doming in the central part of the channel indicates a cyclonic circulation (Fig. 2*c*). This doming is a major feature since it indicates the presence of relatively deep (dense) waters at upper levels. Also important is the fact that isohalines (as well as isotherms and isopycnals) outcrop at the surface in the centre of the channel. These patterns are preliminary indications of possible upward vertical motions at this location. The geostrophic velocity field (Fig. 2*d*) indicates an energetic baroclinic jet flowing northward in the along-channel direction. Maximum velocities within the jet are found at the surface (35 cm/s). On the western side, velocities are low and oriented southward. An important observation is the asymmetric structure of the jet: horizontal and vertical shears are increased at the cold side of the jet and correspond to enhanced cyclonic vorticity. Simulations of the circulation of an unstable front by a primitive equations model showed this pattern to be characteristic of intense upward vertical motions (Wang, 1993).

Horizontal maps

Horizontal fields were objectively analysed on to a 4-km x 4-km regular grid. We used the successive corrections procedure described by Pedder (1993). The characteristic scale (Ls) of this objective analysis scheme, which was set up to 20 km in the present case, determines the degree of smoothing of the output fields. By smoothing the structures with scales shorter than 20 km, we sought to reduce the bias due to the shortest irrelevant scales. Effectively, in the context of this 4-day survey, the shortest structures (< 20 km) have to be considered as highly transient features that are undoubtedly misrepresented by the time and space scales of the sampling. They are thus irrelevant for the purpose of this study, which focuses on the circulation specifically associated with the front and the main eddy. However, the sensitivity of our results to the choice of Ls will be further discussed. Analyses were performed independently at horizontal 10-metre intervals (10, 20,..., 250 m). At 40 m (thermocline), the residual mean square (r.m.s) in stations between the analysed and original density data is 0.4 σ-t units. Dynamic height (with its associated geostrophic velocity field) and salinity maps are plotted at 5 m and 100 m (Fig. 3*a-d*).

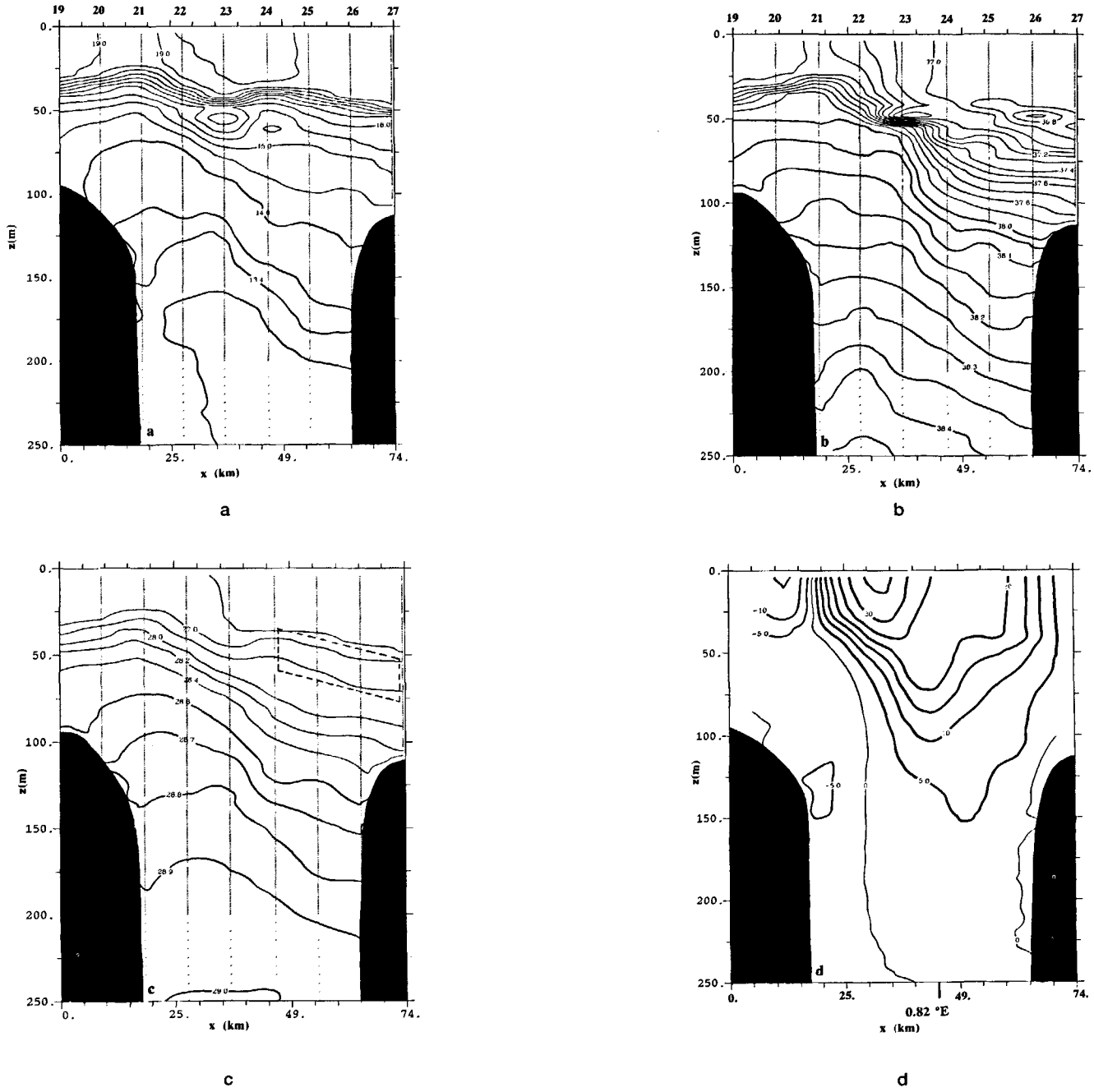

Figure 2

Cross-channel vertical sections at transect 03.

a - Temperature. Contour interval = 0.1 (T<13.5 °C) and 0.5 (T>13.5 °C).

b - Salinity. Contour interval =0.1 psu (S < 38 psu) and 0.05 psu (S > 38 psu).

c - σ-t. Contour interval = 0.5 (σ-t<28.0), 0.2 (28.0<σ-t<28.6) and 0.1 (σ-t>28.6) s-t units. A set of isopycnals centred at 50 m depth has been selected for computation of the isopycnic slope α_x in the cross-channel (or cross-front) direction.

d - Northward geostrophic velocity (/250 m). Contour interval = 5 cm.s^{-1}.

At 5 m, the circulation in the channel is the result of an eddy/front system (Fig. 3*a-b*). The velocity field shows that on the eastern side, MAW (S<37.25 psu) are advected northward within the jet at velocities up to 40 cm.s^{-1} at the surface. A cyclonic eddy, 20-30 km in diameter, is observed in the western part of the channel and is characterized by lower velocities. Waters involved in this re-circulation are quite homogeneous (37.25<S<37.30 psu).

At 100 m, a difference is observed between the salinity and dynamic height distributions (Figure 3*c-d*). At the northern limit of the survey, the eddy is closed in the dynamic height field and open in the salinity field. Bias in the level of no motion or ageostrophic circulation are the most likely explanations for this discrepancy. In any case, the eddy/front structure is found down to 250 m depth (not shown), suggesting a strong vertical coherence of this feature.

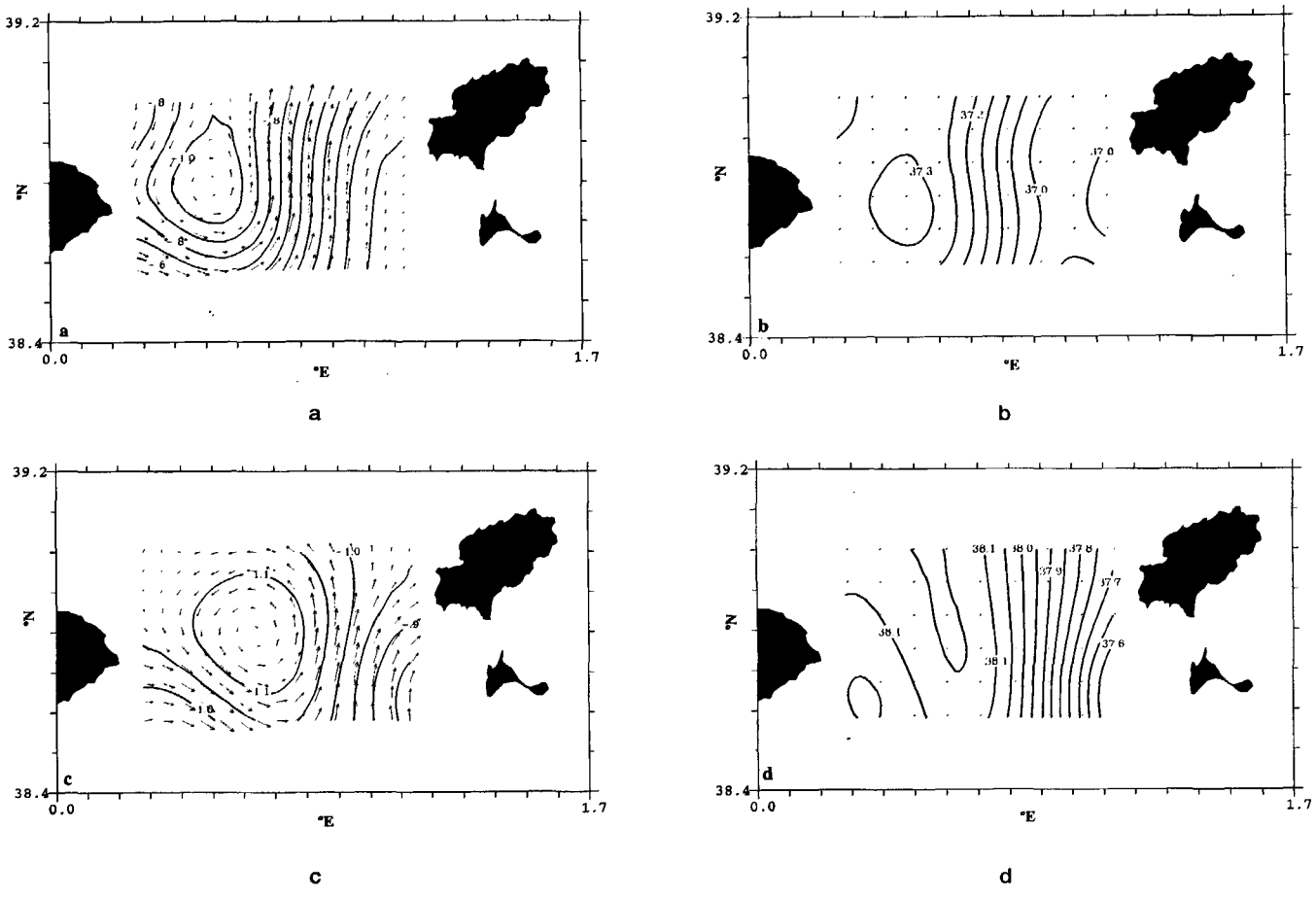

Figure 3

Horizontal maps

a - Dynamic height and geostrophic velocity (/250 m) at 5 m. Contour interval = 0.1 dyn dm. Maximum vector = 39 cm.s^{-1}.
b - Salinity at 5 m. Contour interval = 0.05 psu.
c - Dynamic height and geostrophic velocity (/250 m) at 100 m. Contour interval = 0.05 dyn dm. Maximum vector = 11 cm.s^{-1}.
d - Salinity at 100 m. Contour interval = 0.05 psu.

The ageostrophic motion

A qualitative estimation of the vertical motion

The most commonly used argument for diagnosing vertical motions in the ocean is the conservation of potential vorticity. According to this conservation law, valid in a frictionless ocean without any vorticity source or sink, a water column whose absolute vorticity decreases must be vertically compressed, implying upward vertical motion at its base. Reciprocally, a water column whose absolute vorticity increases is stretched, implying downward velocities at its base. The small geographical extension of the Channel of Ibiza means that changes in planetary vorticity are negligible and permits reasoning on relative vorticity changes only instead of absolute vorticity.

The geostrophic relative vorticity, ξ_g, was calculated by second-order differencing of the analysed dynamic height field. It is represented at 5 m where it has been normalized to the local planetary vorticity f_o (Fig. 4). This ratio is equivalent to the Rossby number, R_0, whose maximum (0.44) is found at the surface. Comparison with the geostrophic circulation at the same depth (Fig. 3*a*) indicates that both fields are not superposable. The main differences occur at the southern edge of the eddy and throughout the front. At the south-western limit of the survey, the flow is due east towards the vorticity maximum (Fig. 4). This corresponds to an increase of the vorticity along the path of the flow; accordingly, downward vertical motions should occur at this location. Conversely, within the front, the northward flow is directed to regions of decreasing vorticity, suggesting upward vertical motion at the front. These vertical motions are characteristic effects of frontogenetic convergence (Hoskins *et al.*, 1985). It is important to bear in mind that relative vorticity includes curvature and shear vorticity. A straight jet presenting only shear vorticity would be characterized by exactly superposable dynamic height and vorticity contours, and hence no vertical motion in the framework of potential vorticity conservation. Thus, curvature is necessary to provide vorticity adjustments where vertical motions can occur. In terms of frontal dynamics, this means that a non-viscous front does not generate vertical motions by itself; only distortions of the front as instability processes are able to trigger upwelling or subduction.

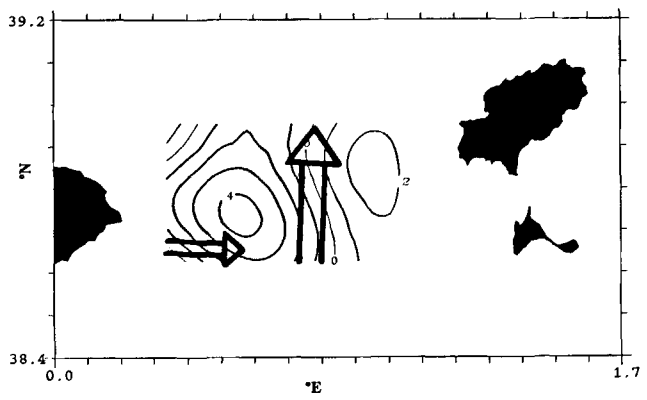

Figure 4

Horizontal map of the geostrophic relative vorticity normalized to the local planetary vorticity (ξ_g/f_0) at 5 m depth. Arrows schematically reproduce the geostrophic circulation of Figure 3a.

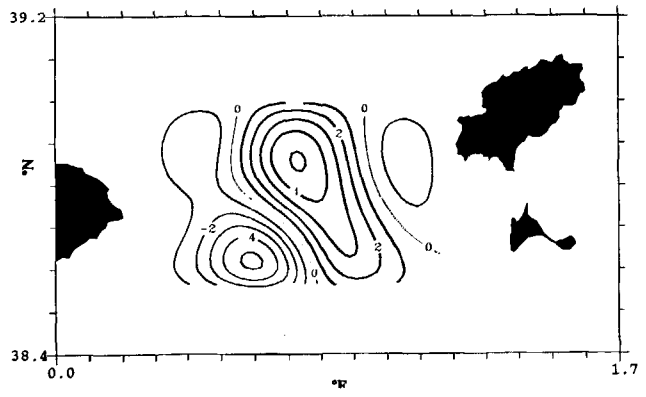

Figure 5

Horizontal distribution of vertical velocity (w) at 95 m as calculated by the omega equation. Contour interval = 10^{-5} m.s^{-1} (w > 0, upward and w < 0, downward).

A quantitative estimation of the vertical velocity: the quasi-geostrophic (QG) omega equation procedure

In the framework of QG theory, the vorticity and thermodynamic equations can be combined to give a diagnostic equation for the vertical motion (omega equation in meteorology) - a formal approach developed by Hoskins *et al.* (1978). A major advantage of this equation is that no assumption for stationarity is required since terms involving time derivatives cancel each other. For oceanic purposes (Leach, 1987; Tintoré *et al.*, 1991), the QG omega equation relates the vertical velocity w to the non-divergent geostrophic motion $V_g = (u_g, v_g)$ and is written as follows:

$$N^2\nabla_h^2 w + f_0^2 \frac{\partial^2 w}{\partial z^2} = 2\nabla.\mathbf{Q} \qquad (1)$$

$$\mathbf{Q} = \frac{g}{\rho_0}\left(\frac{\partial u_g}{\partial x}\frac{\partial \rho'}{\partial x} + \frac{\partial v_g}{\partial x}\frac{\partial \rho'}{\partial y}, \frac{\partial u_g}{\partial y}\frac{\partial \rho'}{\partial x} + \frac{\partial v_g}{\partial y}\frac{\partial \rho'}{\partial y}\right) \qquad (2)$$

where $\nabla_h^2 = \frac{\partial^2}{\partial x^2} + \frac{\partial^2}{\partial y^2}$. The static stability is here considered as a function of z only ($N^2(z)$).

We computed the **Q**-vector within the [0-250 m] layer at levels separated by 10 m from the objectively analysed fields of density (ρ') and geostrophic velocity. Full resolution of the equation requires its inversion. The method we used to invert the omega equation is a relaxation scheme with standard boundary conditions, say w = 0 at surface, bottom (250 m) and four lateral boundaries of the survey.

The result at 100 m is well representative of the vertical velocity patterns throughout the water column (Fig. 5). Maximum velocities are found to the south of the eddy (downward) and within the front (upward), in agreement with the qualitative results derived from the conservation of potential vorticity. Upwelling and subduction present maximum vertical velocities of about 5.10^{-5} m.s^{-1}, say 4 m.day^{-1}. However, maximum subduction is found at the southern limit of the sampling, where some bias may exist in our estimation.

The vertical structure of the vertical velocity field is represented at transect 03 (Fig. 6), so that direct comparison can be made with physical and dynamical properties (Fig. 2*a-d*). The vertical velocity field is characterized by an upwelling pattern which is located at the front and coincides with the strongest horizontal salinity gradients in the

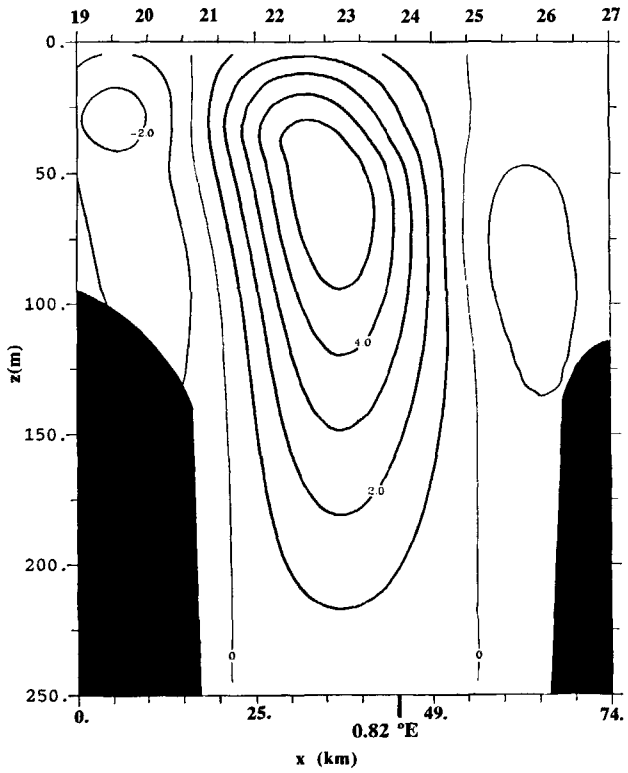

Figure 6

Cross-channel vertical section of vertical velocity (w) at transect 03. Contour interval = 10^{-5} m.s^{-1} (w > 0, upward and w < 0, downward).

middle of the channel (Figure 2*b*). At depth, the upward isohaline doming coincides with the upwelling region in the middle of the channel. It is worth noting that the upwelling maximum is found just below the thermocline (50 m depth) and coincides with a region where isohalines are folded. Also the subduction over the continental slope is associated with a downward tilting of isohalines close to the continental slope. In the upper [0-50 m] layer, upwelling is consistent with surface outcropping isohalines and both subductions coincide with thin homogeneous upper layers located on both sides of the channel. The previously observed asymmetry of the jet (Fig. 2*d*) can also be directly related to the asymmetry (with respect to the jet axis) of the vertical velocity field. Actually, large positive vertical velocities are shifted towards the cyclonic side of the jet.

The three-dimensional ageostrophic motion

The region of strong vertical motions is located in the centre of the channel and direct topographic effects can therefore be neglected. Vertical motions can be interpreted in terms of dynamics of the surface meandering baroclinic jet. A characterization of their nature can be rapidly derived from our previous observations and calculations by starting from the quasi-geostrophic density equation:

$$\frac{\partial \rho}{\partial t} + u_g \frac{\partial \rho}{\partial x} + v_g \frac{\partial \rho}{\partial y} + w \frac{\partial \rho}{\partial z} = 0 \qquad (3)$$

which gives: $w = w_x + w_y + w_t = -\alpha_x u_g - \alpha_y v_g + w_t$ (4)

where:

$$\alpha_x = \frac{\partial \rho / \partial x}{\partial \rho / \partial z},\ \alpha_y = \frac{\partial \rho / \partial y}{\partial \rho / \partial z} \text{ and } w_t = -\frac{\partial \rho / \partial t}{\partial \rho / \partial z} \qquad (5)$$

The sum of w_x and w_y represents the vertical velocity associated with the isopycnic motion of water parcels flowing with the horizontal geostrophic velocities u_g and v_g over sloping (α_x, α_y) isopycnals. w_t is the vertical velocity associated with the vertical displacement of the isopycnal and would be zero in the case of stationary density patterns.

Let us call «along-channel direction», the y axis pointing to the north, which also corresponds to the mean direction of the geostrophic flow within the front (eastern part of the channel) (Fig. 3*a* and 3*b*). «Cross-channel direction» will refer to the x axis pointing to east. We have $u_g << v_g$ since $u_g \approx$ 1-2 cm.s^{-1} while $v_g \approx$ 10-20 cm.s^{-1} in the [0-100 m] layer (Fig. 3*a* and 3*c*). Given the isopycnic slope α_y and our previous calculation of the northward component of the geostrophic velocity v_g (Fig. 2*d*), we can deduce the contribution of the isopycnic vertical velocity w_y in the along-channel direction to the total vertical velocity as estimated by the omega equation. As shown by Figure 7, between 40 and 60 m, isopycnals rise significantly towards the north along the meridian 0.82° E which is a region of the jet characterized by large geostrophic velocities

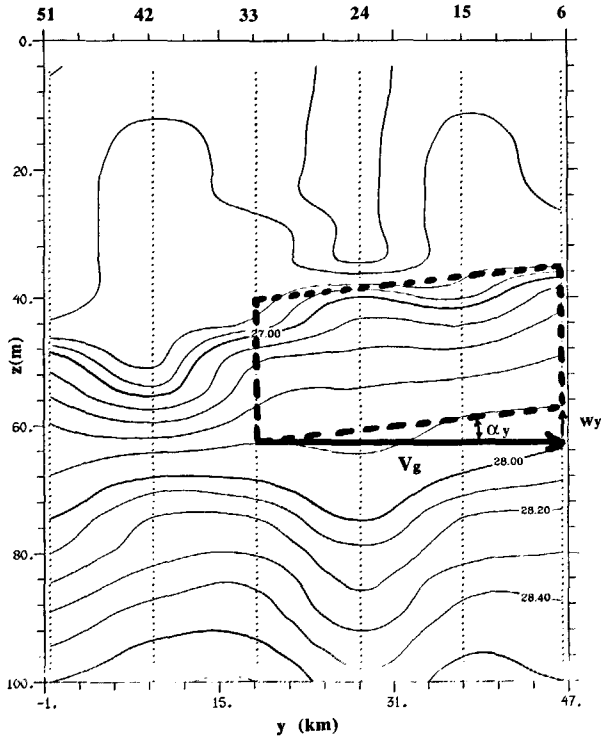

Figure 7

Along-channel vertical section of s–t at 0.82° E. A set of isopycnals centred at 50 m depth has been selected for computation of the isopycnic slope a_y in the along-channel (or along-front) direction.

($v_g \approx$ 20 cm.s^{-1} at 50 m) (Fig. 2*d*). α_y can be estimated from the elevation of isopycnals of Δz = 6 m over a distance of Δy = 28 km as observed at this location. Since $w_y/v_g = \alpha_y = \Delta z/\Delta y$, by considering $v_g \approx$ 20 cm.s^{-1} we obtain $w_y \approx 4\ 10^{-5}$ m.s^{-1}. This value has the same order of magnitude as the total vertical velocity inferred here from the omega equation (Fig. 6). Also at this location, the isopycnic slope α_x is 0.5 10^{-3} (Fig. 2*c*), and by assuming an eastward geostrophic velocity $u_g \approx$ 2 cm.s^{-1}, we obtain $w_x \approx -1\ 10^{-5}$ m.s^{-1}. These results suggest that w_y represents the main contribution to the vertical velocity within the front in comparison with the cross-channel isopycnic vertical velocity (w_x) which is weaker and downward. Those results also suggest that the non-stationary local lifting of isopycnals (w_t) should be weaker than w_y. Thus, the vertical motion is mostly along the uplifting isopycnals in the along-channel direction.

Although the three ageostrophic velocity components can be theoretically recovered from the Q-vector components assuming previous knowledge of adequate boundary conditions, we prefer, for the sake of simplicity and in order to gain more physical insight, to infer them from more basic arguments. Let us focus on the ageostrophic cross-front horizontal velocity by considering the continuity equation:

$$\frac{\partial w}{\partial z} = -\frac{\partial u_{ag}}{\partial x} - \frac{\partial v_{ag}}{\partial y} \qquad (6)$$

Equation (6) tells us that where $\partial w/\partial z$ is positive (resp. negative), the horizontal ageostrophic motion is convergent (resp. divergent). Hence, Figure 6 indicates convergence at the base of the front in the [50-250 m] layer and divergence in the upper [0-50 m] layer. Now, assuming that across-front variations ($\partial./\partial x$) are much larger than those along-front ($\partial./\partial y$), equation (6) can be written:

$$\frac{\partial w}{\partial z} \approx \frac{\partial u_{ag}}{\partial x} \qquad (7)$$

($\partial w/\partial z$) is maximum at the centre of the upwelling cell at x = 37 km on the horizontal axis (Figure 6). For the [50-250 m] layer, this maximum is about $\partial w/\partial z = 2.5\ 10^{-7}\ s^{-1}$. The minimum is reached at x = 55 km and x = 20 km where w = 0 at all depths ($\partial w/\partial z = 0$). A mean value for ($\partial w/\partial z$) within [20-55 km] is thus $1.25\ 10^{-7}\ s^{-1}$. Now, assuming that the horizontal ageostrophic cross-frontal motion u_{ag} is the result of a convergence within the front, we may assume $u_{ag} = 0$ off the front, in the western part of the channel (x = 20 km) where isopycnals are flat (Fig. 2*c*). From $\partial w/\partial z = -\partial u_{ag}/\partial x$, we obtain $u_{ag} = -0.2\ cm.s^{-1}$ at x = 37 km where w is maximum. A better estimation for u_{ag} could be obtained by using an ageostrophic streamfunction (Pollard and Regier, 1992). However, the problem of choosing adequate boundary conditions for u_{ag} remains. In any case, the ageostrophic cross-frontal horizontal velocities ($\approx 0.2\ cm.s^{-1}$) associated with the divergent circulation appear to be lower by one order of magnitude than the cross-channel geostrophic velocities ($ug \approx 2\ cm.s^{-1}$) within the [50-250 m] layer.

For the [0-50 m] layer, since $\partial w/\partial z$ is about five times greater than within the [50-250 m] layer, a similar calculation gives u_{ag}Å 1 $cm.s^{-1}$ showing that u_{ag} has the same order of magnitude than u_g ($\approx 2\ cm.s^{-1}$). A ratio u_{ag}/u_g about 0.5 is consistent with the high Rossby numbers (0.44) found at the surface from the vorticity analysis (Fig. 4) and shows that the [0-50 m] layer is characterized by significant ageostrophic motions.

Sensitivity analysis

To examine the robustness of our estimates of vertical velocity, we carried out the same estimation with a reference level at 150 m instead of 250 m. Neither were the vertical velocity patterns altered (although confined in the top 150 m), nor was their magnitude changed.

Sensitivity of the vertical velocity estimate to the objective analysis characteristic scale was also examined. Instead of Ls = 20 km, we carried out an analysis with Ls = 10 km. Since Ls directly controls the density gradients magnitude and all derived quantities, the **Q**-vector scheme was expected to be largely sensitive to Ls. Actually, with Ls = 10 km, the density and dynamic height maps present short-scale distortions and vertical velocities are found to be one order of magnitude greater (up to 50 $m.day^{-1}$) than for Ls = 20 km. This observation is consistent with the results obtained by Barth (1994) and Strass (1994). Both used a primitive equations numerical model to reproduce vertical motions occurring at frontal instabilities and found that the most intense vertical motions are associated with secondary fluctuations. Though in the context of our 4-day survey these short scales cannot be considered significative due to the lack of synopticity, our result points out the importance of all kinds of frontal instabilities in contributing to vertical transport.

Our relative vorticity and ageostrophic velocity calculations have both established that in the upper 50 m, the Rossby number Ro can be large and reach values up to 0.5. Hence, the use of the QG omega equation scheme in the surface layer is not theoretically valid since the QG assumption (Ro<<1) is not verified. The reliability of the QG omega equation methodology for diagnosing vertical motions at narrow non-quasigeostrophic fronts was checked by Pinot *et al.* (1995). They obtained realistic results for fronts with Rossby numbers up to 0.5, although asymmetry between subduction and upwelling patterns was slightly misrepresented.

In fact, the most arbitrary assumption for the computation of the vertical velocity is the use of homogeneous zero boundary conditions in the inversion of the omega equation. This point is discussed in Pinot *et al.* (1995) who show to what extent the values at the boundaries can affect the solution in the interior of the domain. Generally, for the relaxation scheme we used for the inversion of the omega equation, the influence of the boundaries can be detected only in their vicinity, hence no drastic change in the vertical velocity patterns appears in the interior when modifying the values at the boundaries.

Biological observations

The four nutrient/chlorophyll profiles collected at each transect were used to construct cross-channel vertical sections of the biochemical distributions. For nitrate concentrations (Fig. 8), we observe a general uplift of the nitrocline in the eastward direction (about 25 m between the most western and eastern nitrate stations of the four northern transects 01 to 04). This overall trend indicates that the two water masses that meet and form the front in the Channel of Ibiza have slightly different chemical signatures. MW that enter the channel from the north and further recirculate within the eddy are more oligotrophic than the recent oceanic MAW that flow northward. However, the most interesting feature is a dome pattern located along the 0.82° E meridian (St. 24, 15 and 6). More detailed observation indicates that this doming increases northward. Quantitatively, the base of the nitrocline (3.5 µg – at N – NO_3^- l^{-1}) rises from 90 m to 75 m between transects 03 and 01. This doming is co-located with the centre of the strong upwelling pattern previously diagnosed (Fig. 5). Conversely, there is no doming at the southern transects (Fig. 8*d*), although the cross-channel physical structure of the front is maintained (not shown). This indicates that the nitrate doming is not an intrinsic pattern of the front.

The main pattern that appears on the corresponding cross-channel vertical sections of chlorophyll-*a* concentration (Fig. 9) is the deep chlorophyll maximum (DCM) characteristic of stratified waters (Kiefer *et al.*, 1976) and previously described in the Balearic Sea at this time

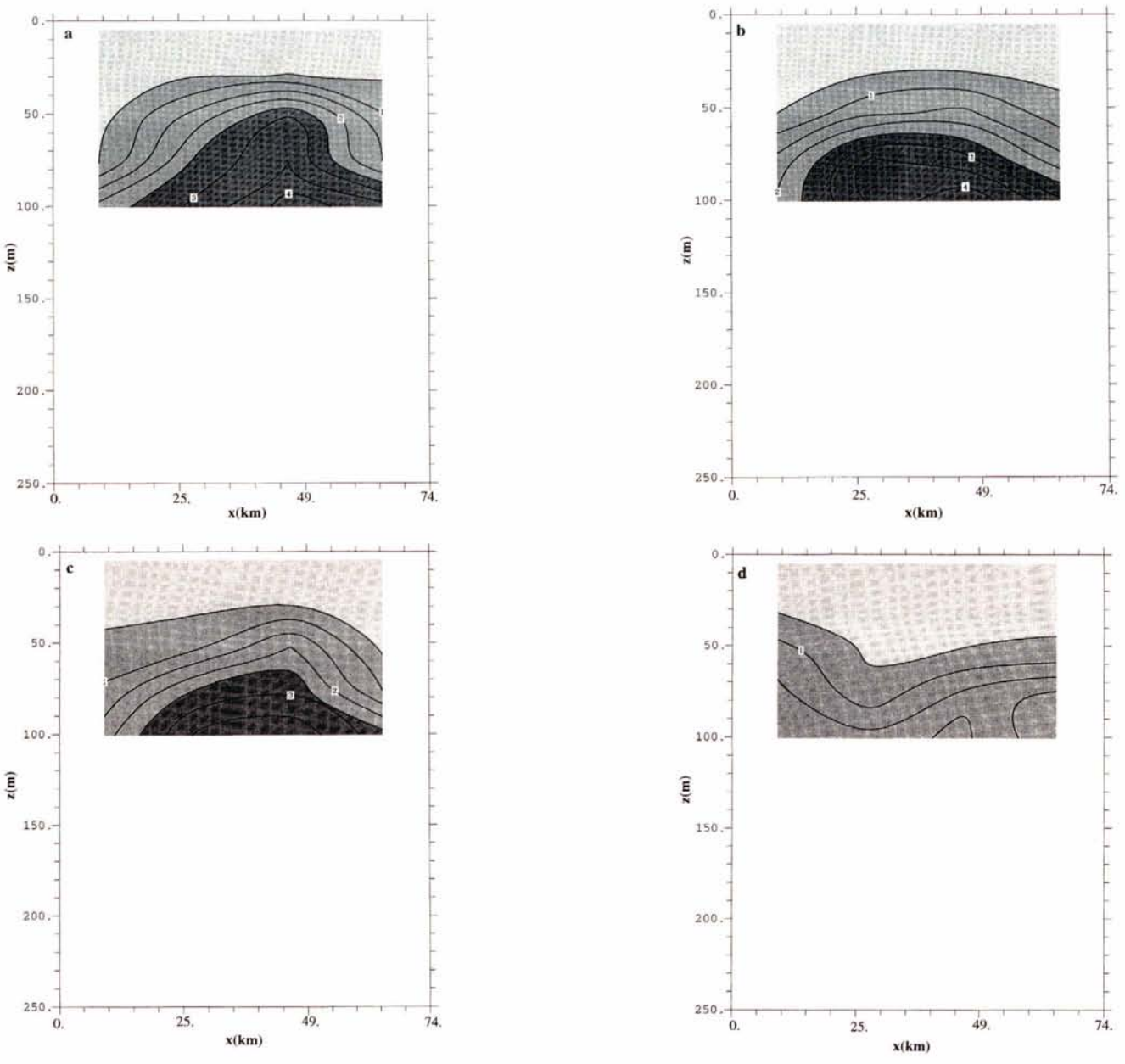

Figure 8

Cross-channel vertical sections of nitrate concentration at transects 01 (a), 02 (b), 03 (c), 04 (d). Contour interval = 0.5 µg – at N – NO_3^- l^{-1}.

of year (Estrada, 1981). However, anomalies of chlorophyll maxima (> 0.5 mg.m^{-3}) are observed at some stations. Most are found within the front and the MAW flow, suggesting an overall correlation between phytoplankton, nutrients and upwelling. Also, some weaker maxima (> 0.3 mg.m^{-3}) are observed in the oligotrophic MW of the cyclonic eddy, coincident with the maximum number of microzooplankton organisms (> 6 n.l^{-1}) found at one station at the surface (Fig. 10).

Impact of the three-dimensional circulation on the biology

Our calculations show that the ageostrophic flow along rising isopycnals in the along-front direction is the major mechanism controlling the transport of deep waters towards the surface within the front. Vertical velocities involved in this mechanism are substantial and reach a few metres per day. Analyses of nitrate data evidence a strong relationship between the upward vertical advection and the doming of the nitrocline at the cold side of the front. We interpret this distortion of the nitrocline as the result of the frontal upwelling which carries nutrient-rich deep waters into the surface layer. Furthermore, this doming increases northward, coincident with the rising isopycnals. Quantitatively, our results show that the net effect of the upward vertical velocities over the nitrate distributions can be measured in terms of a few tens of metres lifting. An observation worth mentioning is that the vertical velocity maximum is coincident with the nitrocline. As a result, upper nitrate concentrations are very sensitive to vertical transport and can be enhanced by a factor of two or three. Enhanced chlorophyll-*a* concentrations, also detected at the same depths, within the DCM, are strongly related to

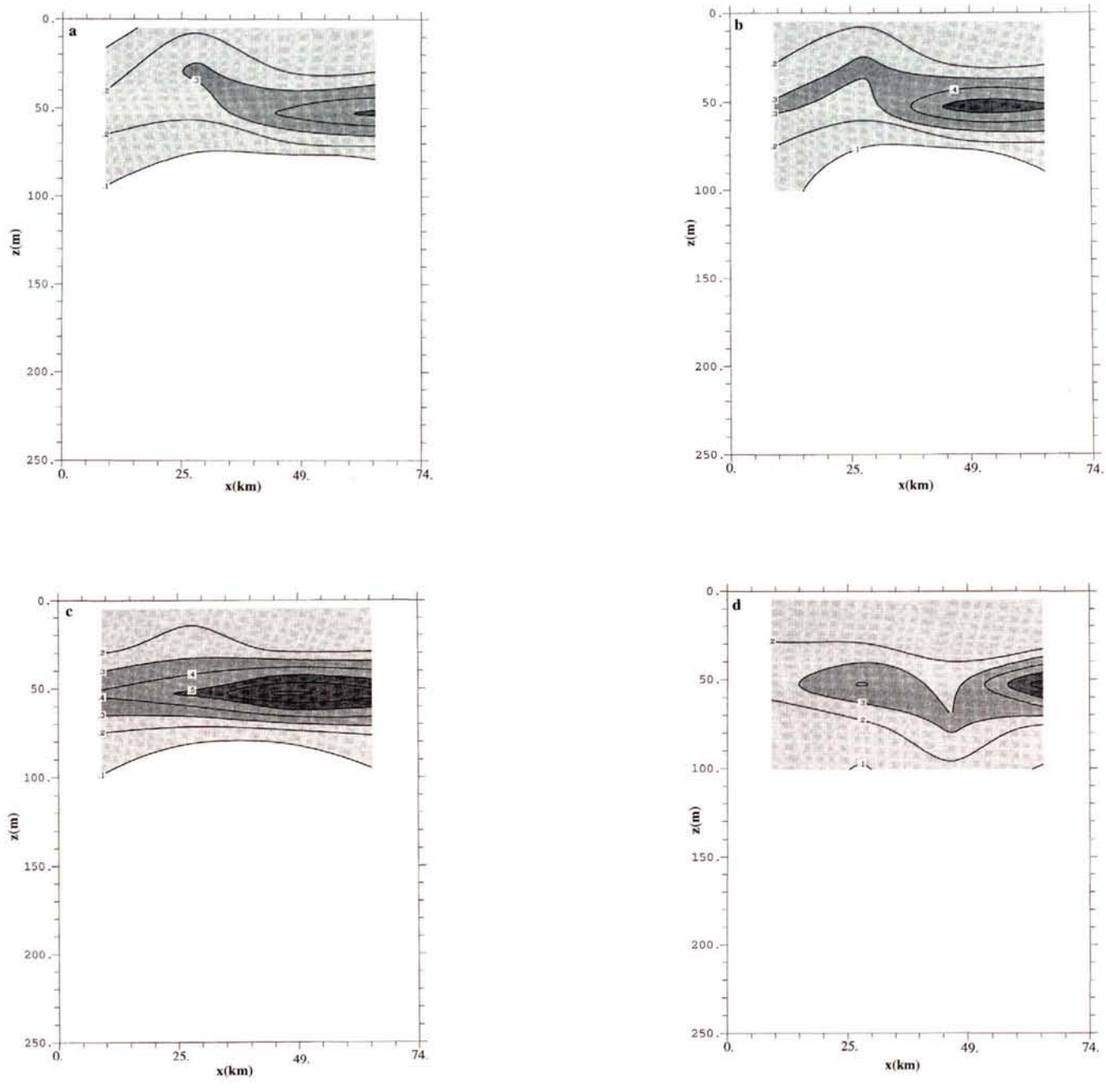

Figure 9

*Cross-channel vertical sections of clorophyll-*a *concentration at transects 01 (a), 02 (b), 03 (c) and 04 (d). Contour interval = 0.1 mg.m^{-3}.*

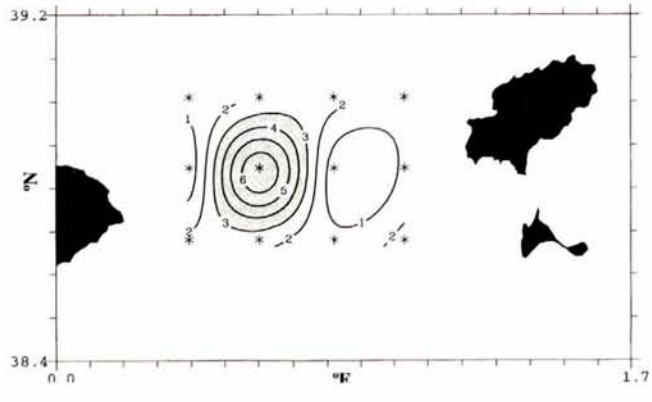

Figure 10

Horizontal distribution of microzooplankton concentration at the surface. Contour interval = 1.0 n.l^{-1} (n=number of individuals).

the nitrocline doming at the cold side of the front. The overall relationship between vertical velocity, nitrates and chlorophyll establishes that frontal upwelling can have a determinant impact on the fertilization of the euphotic layer and further growth of phytoplankton populations.

In addition, we have shown that the frontal upwelling/downwelling is forced by the curvature of the front induced by the adjacent eddy. This eddy plays a determinant role in the circulation of the Channel of Ibiza during the IBIZA-1190 cruise and has strong biophysical implications. Chlorophyll maxima are detected in this eddy as well as a high number of microzooplankton organisms. At this location, the phytoplankton and zooplankton population growth is more likely to be controlled by accumulation processes due to recirculation effects than by fertilization mechanisms. The possible accumulation and the existence of stable conditions within the recirculating eddy can be major factors leading to significant biological species concentrations. Indeed, some researchers believe that fisheries species population structure can be caused by the containment of the early stages of the fish in recirculating eddies (Smith and Morse, 1985). Eddies with adequate time scales that can provide eutrophic conditions for zooplankton growth could be relevant for the general oligotrophic Mediterranean environment.

Before concluding, it is worth noting the paradoxical role played by unstable ocean fronts. On one hand, we have shown that they act as privileged points of exchange where deep waters can supply nutrients to the surface trophic layers. But they can also generate isolated frontal eddies where reduced exchanges provide stable environmental conditions and lead to accumulation of plankton communities. However, the result of our study worth highlighting is the importance of frontal instabilities for the ecosystem of the Channel of Ibiza. Our results quantitatively evidence the impact of mesoscale frontal upwelling on the fertilization of the surface layer. They should be easily extended to the whole Balearic front and to the density fronts of the entire Western Mediterranean. The net effect of vertical circulation on the Mediterranean ecology can be thus expected to be significant. As pointed out above, its experimental determination is based on high resolution surveys with quasi-synoptic mesoscale sampling. However, this methodology lacks the time evolution of the circulation and obviously could not be extended to the whole Mediterranean basin. Thus, the evaluation of the net effect of vertical motions on the ocean ecosystem strongly depends on future frontal and general circulation numerical studies with coupled biophysical models.

Acknowledgments

This work is a UIB/IEO contribution to the PRIMO-0 experiment as part of the EUROMODEL project funded by the E.C. MAST programme (MAS2-CT93-0066) and by the Spanish CICYT (AMB93-1046-CE). Jean-Michel PINOT acknowledges a doctoral E.C. fellowship (ref: MAST-913017) and a post-doctoral fellowship from the Spanish Government (ref: CICYT-SB94-A29028891).

REFERENCES

Armstrong F.A., C.R. Stern, J.D.H. Strickland (1967). The measurement of upwelling and subsequent biological processes by means of the technicon autoanalyzer and associated equipment. *Deep-Sea Res.* **14**, 381-389.

Barth J.A. (1994). Short-wavelength instabilities on coastal jets and fronts, *J. Geophys. Res.* **99**, 16095-16115.

Boucher J., F. Ibanez, L. Prieur (1987). Daily and seasonal variations in the spatial distribution of zooplankton populations in relation to the physical structure in the Ligurian front. *J. Mar. Res.* **45**, 1, 133-173.

Brink K.H., T.J. Cowles (1991). The Coastal Transition Zone Program, *J. Geophys. Res.* 96, C8, 14,637-14,647.

Castellon A., J. Font, E. Garcia (1990). The Liguro-Provençal-Catalan current (NW Mediterranean) observed by Doppler profiling in the Balearic Sea, *Sci. Mar.* **54**, 3, 269-276.

Estrada M. (1981). Biomasa fitoplanctónica y producción primaria en el Mediterráneo Occidental a principios de otoño, *Inv. Pesq.* **45**, 1, 211-230.

Estrada M., R. Margalef (1988). Supply of nutrients to the Mediterranean photic zone along a persistent front, *Oceanologica Acta Spec. Iss.* 133-143.

Fiekas V., H. Leach, K.J. Mirbach, J.D. Woods (1994). Mesoscale instability and upwelling. Part 1: Observations at the North Atlantic Intergyre Front, *J. Phys. Ocean.* **24**, 1750-1758.

Flos J., J. Tintoré (1990). Summer frontal contribution to the fertilization of oceanic waters off the northeast coast of Spain. *Oceanologica Acta* **13**, 1, 21-30.

Font J., J. Salat, J. Tintoré (1988). Permanent features of the circulation in the Catalan Sea, *Oceanologica Acta* **9**, 51-57.

Garcia E., J. Tintoré, J.M. Pinot, J. Font, M. Manriquez (1994). Surface circulation and dynamics of the Balearic Sea, *Coastal and Estuarine Processes* P.E. La Violette Ed. **46**, 73-92.

García-Lafuente J., J.L. López-Jurado, N. Cano Lucaya, M. Vargas-Yañez, J. Aguiar Garcia (1995). Circulation of water masses through the Ibiza Channel, *Oceanologica Acta*, **18**, 2, 245-254.

Grasshof K. (1969). A simultaneous multiple channel system for nutrient analyses in seawater with analog and digital data record. *Technicon International Congress.* Chicago, June 4-6. 133-145.

Hoskins B.J., I. Draghici, H.C. Davies (1978). A new look at the ω-equation, *J. R. Met. Soc.* **104**, 31-38.

Hoskins B.J., M.E. Mc intyre, R.W. Robertson (1985). On the use and significance of isentropic potential vorticity maps, *J. R. Met. Soc.* **111**, 877-946.

Jansa J., O. Reñones, C. Martinez (1992). Fertilization mechanisms in the Ibiza Channel in November 1990, Historia Natural'91, Alemany A. Ed. 297-308.

Kiefer D.A., R.J. Olson, O. Holm-Hansen (1976). Another look at the nitrite and chlorophyll maxima in the Central North Pacific, *Deep-Sea Res.* **23**, 1199-1208.

Leach H. (1987). The diagnosis of synoptic-scale vertical motion in the seasonal thermocline, *Deep Sea Res.* **34**, 2005-2017.

Lhorenz S.E., D.A. Wiesenburg, I.P. De Palma, K.S. Johnson, D.E. Gustafson (1988). Interrelationships among primary production, chlorophyll, and environmental conditions in frontal regions of the Western Mediterranean Sea, *Deep-Sea Res.* **35**, 5, 793-810.

Lindstrom S.S., D.R. Watts (1994). Vertical motion in the Gulf Stream near 68¼ W, *J. Phys. Ocean.* **24**, 2321-2333.

López-Jurado J.L., J.M. García Lafuente, N. Cano Lucaya (1995). Hydrographic conditions of the Ibiza Channel during November 1990, March 1991 and July 1992, *Oceanologica Acta*, **18**, 2, 235-243.

Pedder M.A. (1993). Interpolation and filtering of spatial observations using successive corrections and gaussian filters. *Mon. Wea. Rev.* **121**, 2889-2902.

Pingree R.D., P.M. Holligan, G.T. Mardell (1979). Phytoplankton growth and cyclonic eddies, *Nature* **278**, 701, 245-247.

Pinot J.M., J. Tintoré, D. Gomis (1994*a*). Quasi-synoptic mesoscale variability in the Balearic Sea, *Deep-Sea Res.* **41**, 897-914.

Pinot J.M., J. Tintoré, D.P. Wang (1995). A study about the omega equation for diagnosing vertical motions at ocean fronts, *J. Mar. Res.* (in press).

Pollard R.T., L.A. Regier (1992). Vorticity and vertical circulation at an ocean front, *J. Phy. Ocean.* **22**, 609-625.

Prieur L. (1986). Cross-frontal circulation and production in the Ligurian Sea front (abstr.), *Ecos. Trans. Amer. Geophys. Union* **67**, 981.

Prieur L., A. Sournia (1994). «ALMOFRONT-1» (April-May 1991), an interdisciplinary study of the Almeria-Oran geostrophic front, SW Mediterranean Sea, *J. Mar. Syst.* **5**, 187-203.

Sabates A., J.M. Gili, F. Pages (1989). Relationship between zooplankton distribution, geographic characteristics and hydrographic patterns off the Catalan coast (Western Mediterranean), *Mar. Biol.* **103**, 153-159.

Smith W.G., W.W. Morse (1985). Retention of larval haddock *Melanogrammus aeglefinus* in the Georges Bank region, a gyre-influence spawning area, *Mar. Ecol. Prog. Ser.* **24**, 1-13.

Steedman H.F. (1976). Zooplankton fixation and preservation. UNESCO, Paris, 250 p.

Strass V.H. (1992). Chlorophyll patchiness caused by mesoscale upwelling at fronts, *Deep-Sea Res.* **39**, 1A, 75-96.

Strass V.H. (1994). Mesoscale instability and upwelling. Part 2; Testing the diagnostics of vertical motion with a three-dimensional ocean front model, *J. Phys. Ocean.* **24**, 1759-1767.

Tintoré J., P.E. La Violette, I. Blade, A. Cruzado (1988). A study of an intense density front in the Eastern Alboran Sea: the Almeria-Oran front. *J. Phy. Ocean.*, **18(10)**, 1384-1397.

Tintore J., D. Gomis, S. Alonso, G. Parrilla (1991). Mesoscale dynamics and vertical motions in the Alboran Sea, *J. Phy. Ocean.* **21**, 6, 811-823.

UNESCO (1968). Zooplankton sampling. In: *Monograph. Ocean. Method.* **2**, 174p.

Wang D.P. (1993). Model of frontogenesis: subduction and upwelling. *J. Mar. Res.* **51**, 497-513.